CEAI, Vol.19, No.3 pp. 41-48, 2017 Printed in Romania

Modelling, Validation and Control of Steam Turbine Bypass System of Thermal Power Plant

Yunlong Zhou*, Di Wang*, Tianyu Qi**

** Northeast Dianli University, School of Energy and Power Engineering, China (e-mail: neduzyl@163.com, wd1989125@163.com).*
*** Tsinghua University, Institute of Energy, Environment, and Economy, China (e-mail: qitianyu@mail.tsinghua.edu.cn)*

Abstract: Steam turbine bypass system, as an important auxiliary equipment of thermal power unit, plays a vital role in the process of start-up, shut-down, load rejection and rapid load changes. Temperature of bypass system affects the normal operation directly. In order to study the bypass temperature dynamics, a dynamic model of high-pressure bypass system is established in this paper. The model is verified by fast cut back (FCB) field test data. The results show that the mathematical model has high degree of accuracy. Meanwhile, to solve the bypass over-temperature problem during FCB, an improved control technology is proposed. The controller is basing on static feed-forward compensation control (FCC) and linear active disturbance rejection control (LADRC). Simulation results show that the improved control technology is better over the traditional controller. The optimal value of compensation coefficient of LADRC+FCC is 0.25 in this paper, which provides reference for the bypass control.

Keywords: bypass system, thermal power plant, modelling, linear active disturbance rejection control, feed-forward compensation control.

1. INTRODUCTION

In recent years, with the increasing requirement of load suitability, thermal power unit has to be more efficient in operation. Intermediate reheating units have been widely used due to the high efficiency, which also brings a series of problems, when unit is in the low load or load rejection process. Field operation shows turbine bypass system can solve these problems, while improving the flexibility of plant operation and unit adaptation in the power grid (Krüger et al., 2001).

Fast cut back (FCB) technology of thermal power unit can quickly reduce power load to plant-level to ensure quick restoration after power grid accidents being released. In FCB process, the main steam valve closes quickly and the bypass valve opens quickly. A large number of high temperature and pressure superheated steam gets into the bypass system. If cooling water input flow rate is too slow, the over-temperature protection of bypass system will be triggered, which will shut down the bypass valve. On the contrary, if the bypass cooling water flow rate is too high, it is likely to cause bypass outlet steam mixing with water, which will damage the re-heater (Jin et al., 2006). In addition to FCB, when the thermal load of boiler is higher than the turbine load command, the control system will quickly put bypass into use, so the bypass temperature control system is very important.

In order to study the control technology of thermal power plant, it is necessary to ensure the accuracy of mathematical model. Recently, many achievements have been made in thermal system modelling. A simple dynamic model for a 160 MW oil-burning natural circulation boiler was established, the model reflected the drum pressure, drum water level and the steam flow rate in the riser (Åström and Eklund, 1972; Åström and Bell, 2000). DeMello developed a nonlinear model for the coordinated control system based on thermodynamic analysis method, and the natural circulation boiler dynamic mathematical model concluded two nonlinear models (DeMello, 1991). According to the artificial neural network, took plant boiler data as the training sample, and the steam pressure, temperature, etc. as the outputs of the prediction samples, Smrekar et al. established a high accurate prediction model (Smrekar et al., 2009). Chaibakhsh et al. built steam turbine and boiler model, that was linearized, constructing the form of the transfer function and the simulation study was carried out by Matlab (Chaibakhsh and Ghaffari, 2008; Chaibakhsh et al., 2007). Edge et al. connected the one-dimensional steam-water model of natural circulation boiler with three-dimensional furnace model, and the height regression function of furnace based on the three-dimensional furnace model was the input of the one-dimensional steam-water model (Edge et al., 2011). Sedić et al. divided the riser of natural circulation boiler into four parts, the model can calculate drum water level online, and get pressure distribution of the riser (Sedić et al., 2014). Oko et al. established a 500MW unit boiler-turbine model which can simulate a wide range of variable conditions (Oko et al., 2015). Moreover, Oko et al. used neural network to establish the boiler drum water level and pressure mathematical model, and the prediction results were accurate (Oko et al., 2014).

Aiming at the special working conditions, a great number of results have been obtained. Taylor et al. established a natural circulation boiler model, which considered the thermal stress, and optimized the natural circulation boiler start-up process (Taler et al., 2015). Alobaid et al. established a model of sub-critical three-pressure-stage heat recovery steam generator (HRSG) and compared the numerical results of two process programmes (Apros and Aspen Plus Dynamics) during start-up (Alobaid et al., 2014; Alobaid et al., 2015). Alobaid et al. also built up a Benson HRSG, and analysed the fast start-up procedure (Alobaid et al., 2012). Mertens et al. built up a model of triple-pressure combined-cycle plant and researched the dynamic characteristics of hot start-up and shutdown procedure (Mertens et al., 2016). Eitelberg et al. built up a mathematical model of water circulation system of once-through boiler, and researched the feed water control strategy during start up (Eitelberg et al., 2004). Sindareh-Esfahani et al. characterized the essential dynamics of the HRSG during cold start-up, the dynamic equations of all HRSG's components are developed based on energy and mass balances. Related researches on turbine bypass system have made some achievements (Sindareh-Esfahani et al., 2014). Wang et al. realized 300MW steam turbine IP start-up process by changing the bypass system control logic to study the impact of bypass system on the unit parameters (Wang et al., 2011). Luca Pugi et al. set up a simple steam turbine mathematical model and simulated bypass system operating parameters under different control strategies (Galardi et al., 2014; Pugi et al., 2014; Pugi et al., 2015). Byeon designed a high-pressure bypass control system for a 500MW thermal power unit, ensuring safe operation under special conditions (Byeon, 1997).

Study about thermal power unit modelling provides help for optimization and control. However, research on models for the bypass system is very rare, and research on bypass temperature control system is much fewer.

In this paper, high-pressure bypass system is built up based on the conservation of energy, mass, momentum and the fluid mechanics theory. The model is verified by FCB field test data. Results show that the model is accurate, and it can be used to study the relevant control technology. Moreover, in order to deal with the problem of bypass over-temperature during FCB, the feed-forward compensation controller (FCC) combined with linear active disturbance control (LADRC) is proposed.

2. STEAM TURBINE BYPASS SYSTEM DESCRIPTION

Steam turbine bypass system is a steam system composed of the steam pipeline, temperature reducer and pressure reducer. When the bypass is open, the steam of high parameters can not pass through the steam turbine, but enters the re-heater or condenser. Temperature and pressure reduction device of bypass system is designed to protect re-heater and condenser.

The function of bypass system is as follows:

(1) Improve the start-up performance of the thermal power unit,

(2) Adjust the unit to constant pressure and sliding pressure operation requirements,

(3) Protect the re-heater,

(4) Quickly open the bypass system, reduce pressure, discharge, enable the unit's over-pressure protection and recycle working fluid when the main steam or re-heated steam pressure exceeds predetermined value,

(5) Achieve the function of fast cut back.

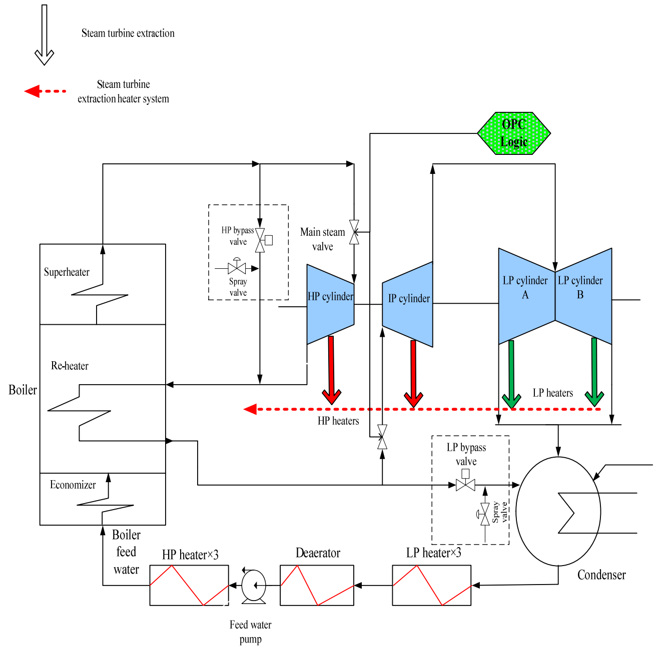

Fig. 1. Structure diagram of thermal power plant.

There are three types of bypass system of large intermediate reheating units: one-order large bypass system, two-order system and three-order system bypass. Considering the unit start-up and running reliability, bypass system should never be close to the turbine.

The study object in this paper is a 300 MW thermal power plant. The main steam pressure is 17 MPa and temperature is 537 ℃ under the rated condition, the bypass system is two-order type, and the bypass system capacity is 60% boiler maximum continuous rating (BMCR). The structure of the plant is shown as Fig. 1.

The bypass system structure is shown as Fig. 2, which consists of bypass regulating valve and bypass temperature-reducing valve. Take the high-pressure bypass system for example, when high-pressure bypass system is running, the main steam enters into bypass pipe from bypass valve, through decompression section, pressure drop, and then goes through temperature-reducing segment by spray water.

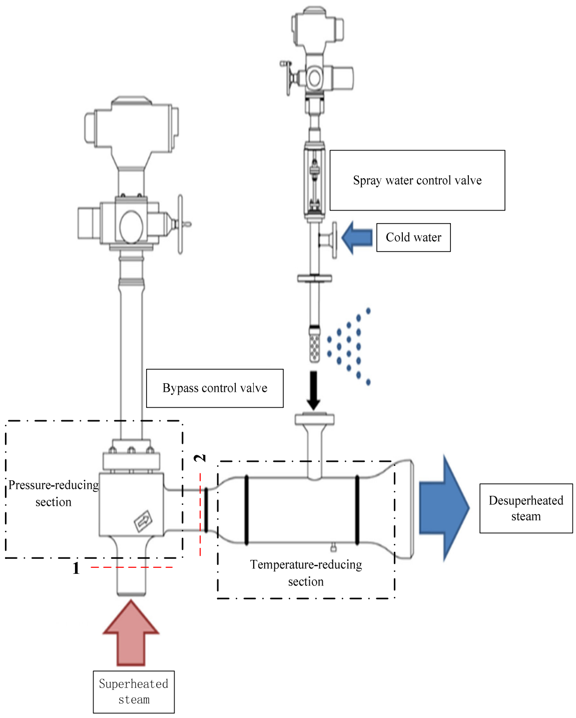

Fig. 2. Typical layout of turbine bypass system (Pugi L. et al., 2015).

3. MODELLING AND VALIDATION

According to the working process, the bypass system can be divided into two sections, pressure-reducing segment and temperature-reducing segment.

In pressure-reducing section, heat exchange with the environment can be ignored during the bypass valve throttling process. The pressure-reducing process can be simplified into basic adiabatic throttling process. In temperature-reducing section, spray water valve controls cooling water flow rate.

3.1 Bypass modelling

3.1.1 Pressure-reducing section

For adiabatic throttling process, steam pressure difference occurs when it flows through the inner tube of the throttling element, but the enthalpy around throttle will not change. According to the adiabatic throttling process, take the front throttle and the rear of throttle as reference surfaces, as shown surface 1 and 2 in Fig. 2. The mathematical model is built up basing on energy equation, continuity equation, and adiabatic equation.

(1) Energy equation

$$\frac{P_1}{\rho_1}\frac{\gamma}{\gamma-1}+\frac{s_1^2}{2}=\frac{P_2}{\rho_2}\frac{\gamma}{\gamma-1}+\frac{s_2^2}{2} \tag{1}$$

(2) Continuity equation

$$A_1 s_1 \rho_1 = A_2 s_2 \rho_2 \tag{2}$$

(3) Adiabatic equation

$$\frac{P_1}{\rho_1^{\gamma}}=\frac{P_2}{\rho_2^{\gamma}} \tag{3}$$

Relationship among the flow rate, pressure, density and other parameters of bypass system can be obtained by the Eq. (1)-Eq. (3), it is shown as Eq. (4).

$$D_{HPbypass}=\frac{\pi}{4}d^2\sqrt{\frac{\gamma}{\gamma-1}}\cdot\sqrt{\frac{2(1-\lambda^{\frac{\gamma-1}{\gamma}})\Delta P\rho_1}{(1-\lambda)(\lambda^{-\frac{2}{\gamma}}-\beta^4)}} \tag{4}$$

where, P, s, A respectively represent pressure, flow velocity, and reference surface cross-sectional area; $D_{HPbypass}$ is the bypass valve inlet flow rate; γ is the adiabatic coefficient; d is the throttle flow diameter; β is the ratio of throttle flow diameter and pipe diameter; ρ is the fluid density; λ is the ratio between front throttle pressure and the rear pressure of the throttle, namely P_1/P_2.

3.1.2 Temperature-reducing section

The basic principle of temperature-reducing is spraying the cooling water to superheated steam flow directly, and cooling water absorbs heat from the superheated steam so that the temperature of the steam can be reduced to the target value, which belongs to the two-phase mixing heat transfer process.

According to the mass and energy balance laws, the following equations can be obtained:

(1) Mass balance equation:

$$D_{out}=D_{HPbypass}+D_w \tag{5}$$

(2) Energy balance equation:

$$D_{out}h_{out}=D_{HPbypass}h_g+D_w h_w+Q_m \tag{6}$$

where, D_{out} is the bypass valve outlet flow rate; D_w is the spray water flow rate; h_g is the main steam enthalpy; h_w is the spray water enthalpy; h_{out} is the bypass valve outlet steam enthalpy; Q_m is friction loss, due to the bypass system along the entire distance is very short, so friction loss is negligible.

Because the temperature reducer outlet steam density changes with the variation of inlet water injection quantity, so it cannot be assumed as a constant. The temperature reducer mathematical model is simplified basing on the principle of two-phase flow, the mass balance equation can be converted as Eq. (7).

$$V\frac{d\rho}{dt}=D_{HPbypass}+D_w-\rho(D_{HPbypass}+D_w)\rho_i^{-1} \tag{7}$$

where, V is attemperator volume, and

$$\rho_i=\frac{\rho_g\rho_w(D_{HPbypass}+D_w)}{D_{HPbypass}\rho_w+D_w\rho_g} \tag{8}$$

Eq. (6) can be transformed as Eq. (9),

$$\frac{dh_{out}}{dt}=\frac{D_{HPbypass}h_g+D_w h_w-(D_{HPbypass}+D_w)h_{out}}{\rho V} \tag{9}$$

where, ρ_g is the main steam density; ρ_w is the spray water density.

3.1.3 Bypass valve inlet steam flow rate

According to the operation parameters of plant, the high pressure bypass flow rate fitting formula is shown as Eq. (10).

$$D_{HPbypass}=0.01\cdot f_1(\mu_V)\cdot f_2(P_m)\cdot\sqrt{T_0/T_m} \tag{10}$$

where,

$$f_1(\mu_V)=0.009356\mu_V^2+0.09543\mu_V-0.4392 \tag{11}$$

$$f_2(P_m)=36.83P_m \tag{12}$$

where, T_0 is 540℃, T_m is the main steam temperature, μ_V is bypass valve opening, and P_m is the main steam pressure.

The relationship between bypass valve opening and position is shown as Fig. 3, and the relationship between main steam pressure and bypass flow rate is shown as Fig. 4.

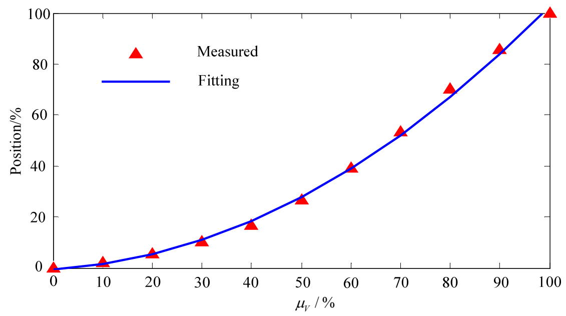

Fig. 3. Relationship between bypass valve opening and position.

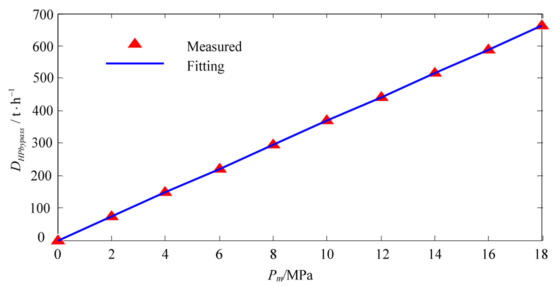

Fig. 4. Relationship between main steam pressure and bypass flow rate.

3.2 Model validation

In order to verify the model built up in this paper, FCB process field data is chosen. In general, the PID controller is widely used in the temperature control in the rear of bypass valve, and the structure of it is shown as Fig. 5, where the bypass temperature is set as 320℃. The model inputs are high-pressure bypass valve opening, main steam pressure, main steam temperature and temperature reduction high-pressure bypass valve opening, as shown in Fig. 6.

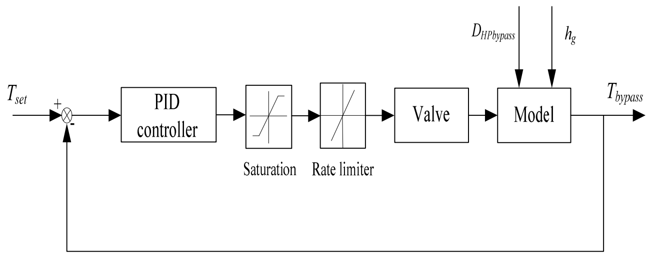

Fig. 5. Control system of bypass temperature reducing.

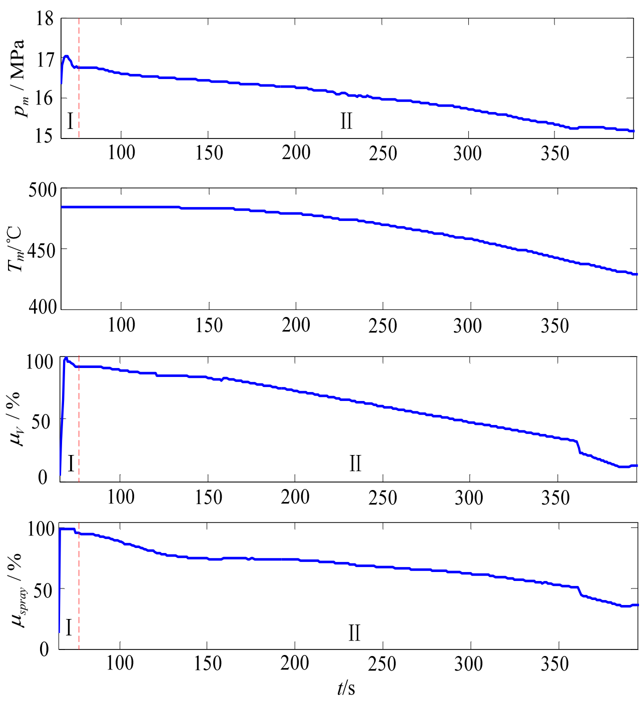

Fig. 6. Mathematical model inputs.

In Fig. 6, the part I curve is the fast-action section, part II curve is the slow-action section. The main reason is that the main steam valve quickly closed since the turbine over-speed protection controller (OPC) operation quickly. The bypass valve temperature-reducing valve is quickly opened, and then bypass system controls the main steam pressure change slowly.

The verification results are shown as Fig. 7, by which the field test data is accord with model output curves very well. Therefore, bypass system mathematical model established in this paper is correct, and it can be used to study the temperature control technology.

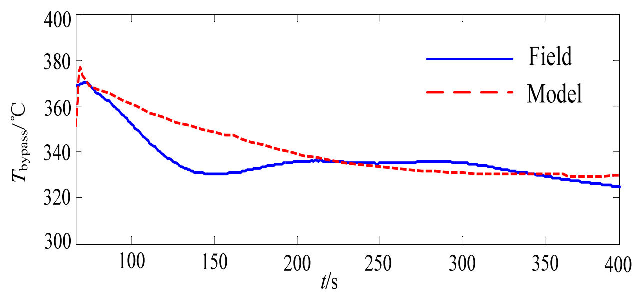

Fig. 7. Mathematical model validation result.

4. BYPASS TEMPERATURE CONTROL

4.1 Active disturbance rejection control

To deal with the shortcomings of PID controller, Han proposed active disturbance rejection control (ADRC), which composed of three parts: tracking differentiator (TD), extended state observer (ESO), non-linear state error feedback (NLSEF) (Han, 1995; 1998; 2002; 2007). However, it is not easy to adjust so many parameters, thus its application in engineering is limited. Gao proposed the linear active disturbance control (LADRC) by linearization techniques of three parts of ADRC, and good control effect was obtained (Gao, 2003).

The idea of LADRC is based on the theory of ADRC, however, there are obvious differences between the two controllers.

(1) ADRC involves tracking differentiator (TD) to enable the tracking signal inputs v_1 and differential form v_2. In LADRC, assuming LADRC observation is accurate, then v_1, v_2 can be estimated directly from LESO, its structure is simple, it is easier to implement.

(2) The ESO is transformed from the original third order nonlinear form into the multi-order state space realization form, which improves the accuracy and the bandwidth.

(3) NLSEF law is used in ADRC, however, linear control law is applied in LADRC, and it is easier to be achieved.

In general, the second-order system

$$\ddot{y} = bu + f(\dot{y}, y, u, \mathrm{d}) \tag{13}$$

where, b is the process parameter with estimation value of b_0, and f ( ) is the total disturbance, including the unmodelled dynamics in system and external disturbance d. The state space equation from Eq. (13) can be rewritten as:

$$\begin{cases} \dot{x}_1 = x_2 \\ \dot{x}_2 = b_0 u + x_3 \\ \dot{x}_3 = h \\ y = x_1 \end{cases} \tag{14}$$

where, $x_1 = y$, $x_2 = \dot{y}$, $x_3 = f(\dot{y}, y, u, \mathrm{d})$, and $h = \dot{f}(\dot{y}, y, u, \mathrm{d})$.

In order to estimate the value of y, $\dot{y}$, and $f(\dot{y}, y, u, \mathrm{d})$, the ESO is given by

$$\begin{cases} \dot{z} = A_0 z + B_0 u + L_0(y - \hat{y}) \\ \hat{y} = C_0 z \end{cases} \tag{15}$$

where, $A_0 = \begin{bmatrix} 0 & 1 & 0 \\ 0 & 0 & 1 \\ 0 & 0 & 0 \end{bmatrix}$, $B_0 = \begin{bmatrix} 0 \\ b \\ 0 \end{bmatrix}$, $C_0 = [1 \ \ 0 \ \ 0]$, $\hat{y}$ is the estimation value of output y, $z = [\mathrm{z}_1 \ \ \mathrm{z}_2 \ \ \mathrm{z}_3]^T$ is the state vector in ESO, representing the estimation value of $x = [x_1 \ \ x_2 \ \ x_3]^T$. L_0 is the observer gain vector, which can be selected appropriately by using the pole-placement method. Then the tuning process has been simplified. The observer gains are parameterized as follows:

$$L_0 = [\beta_1, \beta_2, \beta_3]^T = [3\omega_0, 3\omega_0^2, \omega_0^3]^T \tag{16}$$

The LESO of LADRC can be written as:

$$\begin{cases} \dot{z}_1 = z_2 + \beta_1(y - z_1) \\ \dot{z}_2 = z_3 + \beta_2(y - z_1) + b_0 u \\ \dot{z}_3 = \beta_3(y - z_1) \end{cases} \tag{17}$$

where, b_0 is the estimation value of b; β_1, β_2, β_3 are the observer parameters; ω_0 is observer bandwidth.

After obtaining $\hat{f}$, the estimation of $f(\dot{y}, y, u, \mathrm{d})$, LADRC can cancel it in the control law, $u = \frac{-\hat{f} + u_0}{b_0}$. Then the original plant can be reduced to a unit-gain double integrator plant can by ignoring the estimation error in z_3:

$$\ddot{y} = (f(\dot{y}, y, u, \mathrm{d}) - \hat{f}) + u_0 \approx u_0 \tag{18}$$

The PD control law is:

$$u_0 = k_p(r - z_1) - k_d z_2 - z_3 \tag{19}$$

The values of the gains k_p and k_d can be selected to place all the closed-loop poles at ω_c, where, ω_c is the controller bandwidth, and $k_p = \omega_c^2$, $k_d = 2\omega_c$. The structure of LADRC is shown as Fig. 8.

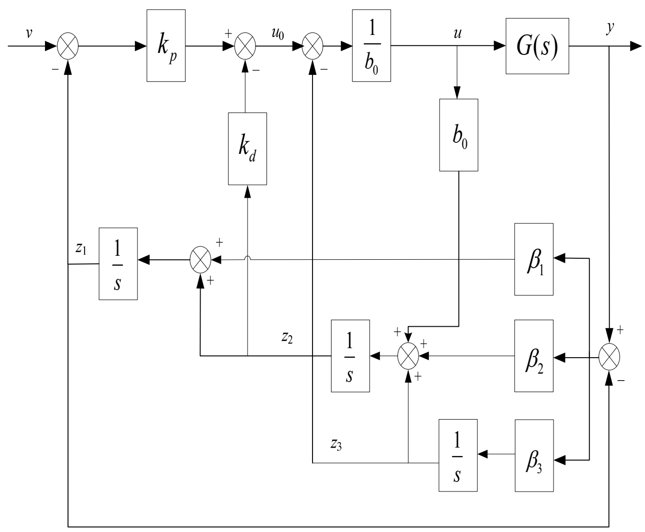

Fig. 8. Structure of LADRC

4.2 Static feed-forward compensation control

Due to the operation speed of bypass cooling system directly affects the bypass temperature, fast and accurate temperature control technology can ensure the safe operation of re-heater.

When the bypass valve is open, the main steam will enter into the re-heater, then the temperature of bypass valve will increase, namely the change rate of temperature is much more lower than that of the bypass flow. In order to control the temperature of the bypass system quickly and effectively, bypass flow rate compensation control system is proposed in this paper, which is combined with LADRC.

Feedforward control is mainly applied to the environment of large amplitude and frequent disturbance, and has obvious effect on the controlled variable. When the control channel of the object's lag is large, the feedback control is not timely, the feed forward control can solve the above problems well (Rijlaarsdam et al., 2012; Shen et al., 2013; Luo et al., 2015).

According to the characteristics of the disturbance compensation, feedforward control can be divided into two types: static feedforward and dynamic feedforward. The static feedforward controller adopts proportional control, it has simple structure and is easy to be realized in engineering, but there may be some dynamic deviation. Dynamic feedforward controller is built up based on the invariance principle, the control scheme can significantly improve the quality of the control system, but its structure is more complex, and it is relatively difficult to be realized. Therefore, the static feedforward controller is used in this paper.

The control structure is shown in Fig. 9, where λ_c is the coefficient of static compensator.

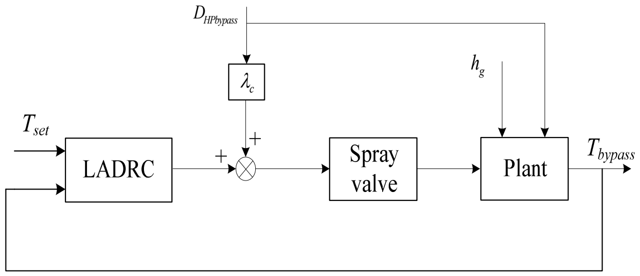

Fig. 9. Structure of feed-forward compensation control.

5. RESULTS AND DISCUSSION

5.1 Related parameters

In order to validate the effectiveness of the controller proposed in this paper, the simulation tests of bypass valve in step change and FCB are carried out, the controller parameters are shown as Table 1.

Table 1. Controller related parameters.

Parameter	Value
ω_0	1.05
ω_c	10.2
b_0	0.002
λ_c	0.1

5.2 Bypass valve opening step change simulation

In order to study the stability of the controller proposed in this paper, the step change simulation tests of bypass valve opening are carried out. The step changes are 50%, 60%, 70% and 80%, the simulation results are shown as Fig. 10.

When the bypass valve is open, the temperature in the rear of bypass valve increases quickly, and then reaches steady state slowly. There is no violent shock appearance. With the increment of step change, the adjustment time is longer.

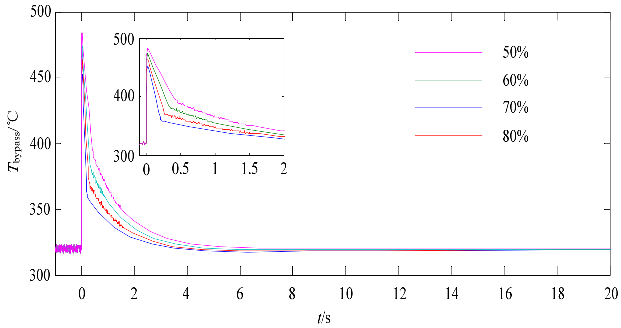

Fig. 10. Simulation results of the step change.

5.3 FCB simulation test

In order to study the performance of the proposed control strategy, FCB simulation tests with different controllers are conducted. These controllers are as follows**:** PID, PID+FCC, LADRC+FCC, LADRC.

Simulation results of FCB process are shown as Fig. 11. PID controller has the worst control performance, LADRC+FCC control performance is the best. The main reason is that, when the bypass flow rate suddenly increases, FCC technology can act timely, and LADRC can effectively restrain the internal and external disturbance. The outputs of LESO are shown as Fig. 12 under LADRC+FCC.

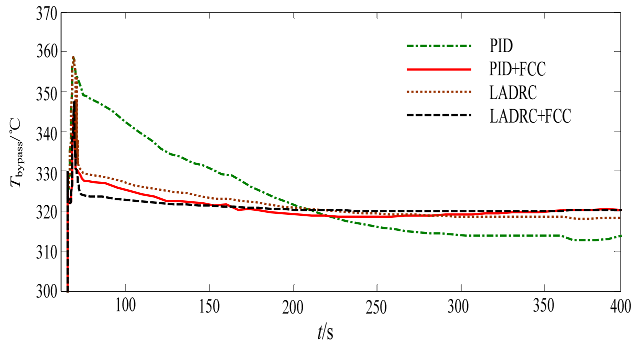

Fig. 11. Simulation results of different controllers.

In order to study the control effect of static forward compensation coefficient of LADRC+FCC, FCB simulation tests under different static forward compensation coefficients are conducted, and the results are shown as Fig. 13. It shows that the greater the compensation coefficient is, the faster the temperature reaches the set value. However, when the compensation coefficient exceeds 0.25, it will cause over compensation leading to the adjustment process is unstable. So the optimal value of compensation coefficient of LADRC+FCC is 0.25 in this paper. For the other types of bypass system, the value can be adjusted according to the actual compensation coefficient of static process.

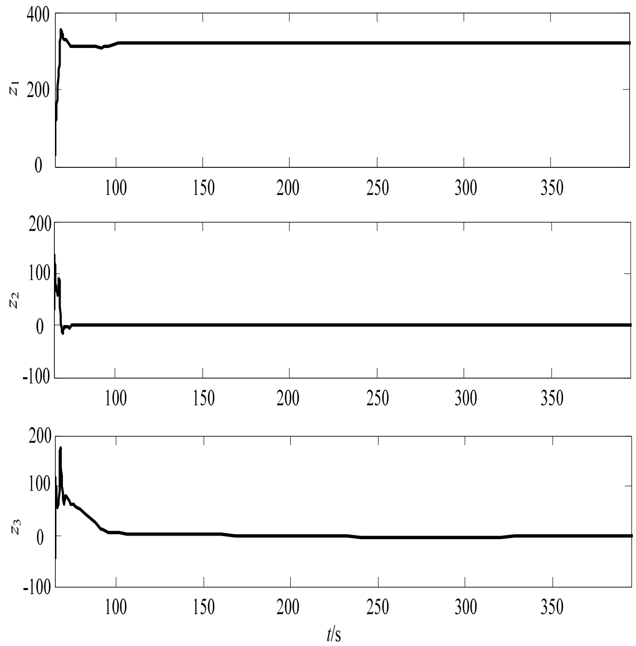

Fig. 12. Outputs of LESO of LADRC+FCC.

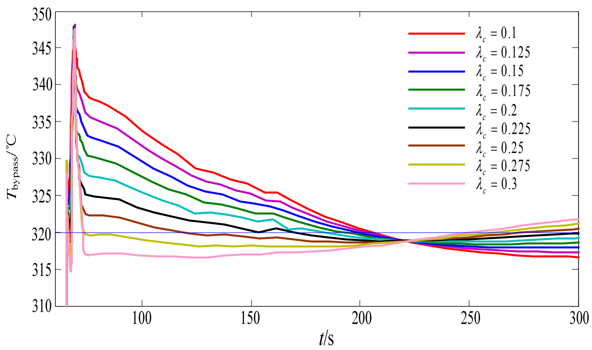

Fig. 13. FCB simulation results of LADRC+FCC under different compensation factors.

CONCLUSIONS

(1) Bypass system is critical to thermal power units, in order to control the temperature in the rear of bypass valve quickly and effectively, a dynamic mathematical model of high-pressure bypass system is established. The model is validated by field test data of FCB with unit operating at 100% BMCR. The results show the model has high accuracy and credibility, which provides a model support for bypass system simulation and control.

(2) To solve the FCB process bypass over-temperature problem, feed-forward compensation combined with linear active disturbance rejection control (LADRC) technology is proposed. Simulation results show the improved controller is better than traditional PID controller and individual compensation controller. The simulation results can provide reference for bypass temperature control under different operating conditions.

ACKNOWLEDGMENT

This research is supported by the Science and Technology Project of China Southern Power Grid (Project No. K-GZ2012-130) and the Science and Technology Development Project of Jilin Province of China (Project No. 20150204017SF).

REFERENCES

Alobaid, F., Karner, K., Belz, J., Epple, B., and Kim H. G. (2014). Numerical and experimental study of a heat recovery steam generator during start-up procedure, *Energy, Vol. 64*, pp. 1057-1070.

Alobaid, F., Pfeiffer, S., Epple, B., Seon, C. Y., and Kim, H. G. (2012). Fast start-up analyses for Benson heat recovery steam generator, *Energy, Vol. 46*, pp. 295-309.

Alobaid, F., Starkloff, R., Pfeiffer, S., Karner, K., Epple, B., and Kim, H. G. (2015). A comparative study of different dynamic process simulation codes for combined cycle power plants – Part B: *Start-up procedure, Fuel, Vol. 153,* pp. 707-716.

Åström, K. J., and Bell, R. D. (2000). Drum-boiler dynamics, *Automatica*, Vol. 36, No. 3, pp. 363-378.

Åström, K. J., and Eklund, K. (1972). A simplified non-linear model of a drum boiler-turbine unit, *International Journal of Control Automation and Systems*, Vol. 16, No. 1, pp. 145-169.

Chaibakhsh, A., and Ghaffari, A. (2008). Steam turbine model, *Simulation modelling Practice and Theory*, Vol. 16, No. 9, pp. 1145-1162.

Chaibakhsh, A., Ghaffari, A, and Moosavian, S. A. A. (2007). A simulated model for a once-through boiler by parameter adjustment based on genetic algorithms, *Simulation modelling Practice and Theory*, Vol. 15, No. 9, pp. 1029-1051.

DeMello, F. P. (1991). Boiler models for system dynamic performance studies, *IEEE Transactions on Power Systems*, Vol. 16, No. 1, pp. 66-73.

Edge, P. J., Heggs, P. J., Pourkashanian, M., and Williams, A. (2011). An integrated computational fluid dynamics–process model of natural circulation steam generation in a coal-fired power plant, *Computers and Chemical Engineering,* Vol. 35, pp. 2618-2631.

Eitelberg, E., and Boje, E. (2004). Water circulation control during once-through boiler start-up, *Control Engineering Practice*, Vol. 12, No. 6, pp. 677-685.

Galardi, E., Pugi, L., Lucchesi, N., and Rindi, A. (2014). Hardware in the loop testing of a steam turbine bypass regulator using a TI C2000 micro-controller, *Proc. 6th Int. European Embedded Design in Education and Research Conference*, pp. 255-259.

Gao, Z. Q. (2003). Scaling and bandwidth-parameterization based controller tuning, Proc. *IEEE Int. Conf. American Control, Denver*, pp. 4989-4996.

Han, J. (1995). The ''Extended State Observer'' of a class of uncertain systems, *Control and Decision*, Vol. 10, No. 1, pp. 85-88.

Han, J. (1998). Auto-disturbance rejection control and its application, *Control and Decision*, Vol. 13, No. 1, pp. 19-23.

Han, J. (2002). From PID technique to active disturbances rejection control technique, *Control Engineering of China*, Vol. 9, No. 3, pp. 13-18.

Han, J. (2007). Auto disturbances rejection control technique, *Frontier Science*, Vol. 1, No. 1, pp. 24-31.

Hwa, W. B., and James, L. U. (1997). Designing a standard thermal power plant for daily startup/shutdown: the HP Bypass control and safety function, *ISA Transactions*, Vol. 36, No. 1, pp. 71-77.

Jin, W., Li, M., and Zhang, H. (2006). Fast cut back capability of large fossil fired power units, *Journal of Power Engineering,* Vol. 26, No. 4, pp. 520-524.

Krüger, K., Rode, M., and Franke, R. (2001). Optimal control for fast boiler start-up based on a nonlinear model and considering the thermal stress on thick-walled components, *Proc. IEEE Int. Conf. Control Applications*, Mexico City, pp. 570-576.

Luo, Y., Zhang, T., Zhou, L., and Chen, Y. (2015). Prefiltering and head-dependent adaptive feed-forward compensation for translation vibration in hard-disc-drive, *Mechatronics*, Vol. 27, pp. 13-19.

Mertens, N., Alobaid, F., Lanz, T., Epple, B., and Kim, H. G. (2016). Dynamic simulation of a triple pressure combined-cycle plant: Hot start-up and shutdown, *Fuel*, Vol. 167, pp. 135-148.

Oko, E., and Wang, M. (2014). Dynamic modelling, validation and analysis of coal-fired subcritical power plant, *Fuel*, Vol. 135, pp. 292-300.

Oko, E., Wang, M., and Zhang, J. (2015). Neural network approach for predicting drum pressure and level in coal-fired subcritical power plant, *Fuel*, Vol. 151, pp. 139-145.

Pugi, L., Carcasci, C., Galardi, E., Rindi, A., Lucchesi, N. (2014). Real time simulation of a turbine bypass controller, *Proc. 10th IEEE/ASME Int. Conf. Mechatronic and Embedded Systems and Applications*, pp. 1-6.

Pugi, L., Galardi, E., Carcasci, C., Rindi, A., and Lucchesi, N. (2015). Preliminary design and validation of a Real Time model for hardware in the loop testing of bypass valve actuation system, *Energy Conversion and Management*, Vol. 92, No. 1, pp. 366-384.

Rijlaarsdam, D., Nuij, P., Schoukens, J., and Steinbuch, S. (2012). Frequency domain based nonlinear feed forward control design for friction compensation, *Mechanical Systems and Signal Processing,* Vol. 27, pp. 551-562.

Sedić, A., Katulić, S., and Pavković, D. (2014). Dynamic model of a natural water circulation boiler suitable for on-line monitoring of fossil/alternative fuel plants, *Energy Conversion and Management*, Vol. 87, pp. 1248-1260.

Shen, G., Zhu, Z., Zhang, L., Tang, Y., Yang, C., Zhao, J., Liu, G., and Han, J. (2013). Adaptive feed-forward compensation for hybrid control with acceleration time waveform replication on electro-hydraulic shaking table, *Control Engineering Practice*, Vol. 21, No. 8, pp. 1128-1142.

Sindareh-Esfahani, P., Habibi-Siyahposh, E., Saffar-Avval, M., Ghaffari, A., and Bakhtiari-Nejad, F. (2014). Cold start-up condition model for heat recovery steam generators, *Applied Thermal Engineering*, Vol. 65, No. 1-2, pp. 502-512.

Smrekar, J., Assadi, M., Fast, M., Kuštrin, I., and De, S. (2009). Development of artificial neural network model for a coal-fired boiler using real plant data, *Energy*, Vol. 34, pp. 144-152.

Taler, J., Dzierwa, P., Taler, D., and Harchut, P. (2015) Optimization of the boiler start-up taking into account thermal stresses, *Energy*, Vol. 92, pp. 160-170.

Wang, W. B., Wang, X. D., Liu, D. J. (2011). IP start-up control for 300MW turbine unit with bypass system, *Procedia Engineering*, Vol. 16, pp. 493-498.